

J. Chem. Soc., Faraday Trans. 1, 1988, **84**(1), 75–85

Effect of Solvent on the Reactions of Coordination Complexes

Part 2.—Kinetics of Solvolysis of *cis*-(Chloro)(imidazole)bis(ethylenediamine)-cobalt(III) and *cis*-(Chloro)(benzimidazole)bis(ethylenediamine)cobalt(III) in Methanol–Water and Ethylene Glycol–Water Media

Anadi C. Dash* and Neelamadhab Dash

Department of Chemistry, Utkal University, Bhubaneswar 751 004, India

The kinetics of solvolysis of *cis*-(chloro)(imidazole)bis(ethylenediamine)-cobalt(III) and *cis*-(chloro)(benzimidazole)bis(ethylenediamine)cobalt(III) have been investigated in aqueous methanol (MeOH) and aqueous ethylene glycol (EG) media (0–80% by weight of MeOH or EG) at 45–64.7 °C. The logarithm of the pseudo-first-order rate constants for MeOH–water media exhibits linear dependence with the reciprocal of the bulk dielectric constant (D_s^{-1}), the mole fraction of MeOH (X_{MeOH}) and the solvent ionizing power Y ($Y_{1\text{-AdCl}}$) as determined by the solvolysis rates of 1-adamantyl chloride. Similar plots ($\log k_{\text{obs}}^s$ vs. x_{EG} or D_s^{-1}) for EG–water media are non-linear. It is evident that the solvation phenomenon plays dominant role and the rate of solvolysis is mediated by the dual solvent vectors, the overall acidity and basicity of the solvent mixtures. The relative transfer free-energy calculations indicate that the mixed solvent media exert more destabilizing effect on the transition state as compared to the initial state. The activation enthalpy and entropy vs. X_{org} (where X_{org} is the mole fraction of the organic solvent component) plots display maxima and minima indicating that the solvent structural changes play significant role in the activation process. The activation free energy at a given temperature, however, increases only marginally and linearly with increasing X_{org} . The mutual compensatory effect of activation enthalpy and entropy on the activation free energy is in keeping with the fact that the perturbations of the reaction zone and the solvent network remain approximately proportional to each other with increasing X_{org} so that the isodelphic and the lyodelphic components of ΔH^\ddagger and ΔS^\ddagger correlate well with each other.

In a previous paper¹ the kinetics of solvolysis of the *cis*-[Co(en)₂(bzmH)Br]²⁺ (where bzmH = benzimidazole) was reported in methanol–water media over an extended range of solvent composition (0–80% methanol by weight) and at 35–55 °C. The rate data ($\log k_{\text{obs}}^s$) exhibited a marked departure from a linear correlation with the reciprocal of the bulk dielectric constant of the medium and the Grunwald–Winstein parameter, Y , or the revised Y values (for 1-adamantyl chloride) reported by Bentley and Carter.² Attempts to correlate $\log k_{\text{obs}}^s$ with the mole fraction of MeOH (X_{MeOH}) were most successful. Plots of $\log k_{\text{obs}}^s$ vs. X_{MeOH} were excellent straight lines at 50 and 55 °C; however, increasing positive deviation from linearity was noted at lower temperatures. These facts led us to believe that the specific solvation effects presumably become less significant with increasing temperature. The trend in the variation of the activation enthalpy and entropy with X_{MeOH} indicated that the solvent cosphere of the substrates in the initial state (i.s.) and the transition state (t.s.) exerts a significant modulating effect on the rate and the thermodynamic parameters of the solvolysis process.

For the aqueous alcohol system it is normally expected that the interaction of the

solvent with the substrate both in the initial state (i.s.) and the transition state (t.s.) will very much depend upon the acidity and basicity of the leaving groups as well as of the solvent. In this context it was felt worthwhile to extend the solvent-effect studies to other suitable cobalt(III) substrates which can interact favourably with the solvent systems. In this paper we present some of our findings on the kinetics of solvolysis of the *cis*-(chloro)(imidazole)bis(ethylenediamine)cobalt(III) and the *cis*-(chloro)(benzimidazole)bis(ethylenediamine)cobalt(III) ions in methanol–water and ethylene glycol–water media.

Experimental

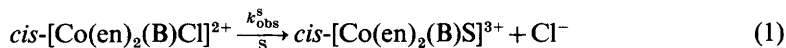
The *cis*-(chloro)(imidazole)bis(ethylenediamine)cobalt(III) diperchlorate and the *cis*-(chloro)(benzimidazole)bis(ethylenediamine)cobalt(III) diperchlorate were prepared and purified as described earlier.^{3,4} The purities of the samples were checked by analysis of Co and Cl⁻ which agreed to better than $\pm 0.1\%$ of the calculated values for the formulae $[\text{Co}(\text{C}_2\text{H}_8\text{N}_2)_2(\text{C}_3\text{N}_2\text{H}_4)\text{Cl}](\text{ClO}_4)_2$ and $[\text{Co}(\text{C}_2\text{H}_8\text{N}_2)_2(\text{C}_7\text{N}_2\text{H}_6)\text{Cl}](\text{ClO}_4)_2$, respectively.

AnalaR methanol and ethylene glycol (EG) were further dried over 4 Å molecular sieve and distilled; the middle fraction was collected. Gas chromatography using an Aimil Nucon model 5700 gas chromatograph did not reveal the presence of other impurities. Solvent mixtures were prepared by weight in the usual way. Spectrophotometric measurements were made using an LKB Biochrom Ultrospec II spectrophotometer or a u.v.–visible spectrophotometer manufactured by the Electronic Corporation of India Ltd.

The procedure for following the kinetics of solvolysis of the complexes and determining the observed pseudo-first-order rate constants (k_{obs}^s) has been described in detail in our earlier paper.¹

Results and Discussion

The ligand-field bands of the chloro complexes are influenced little by the organic solvent components of the mixed solvent media. Successive spectral scans ($400 \leq \lambda/\text{nm} \leq 580$) during the solvolysis of the *cis*- $[\text{Co}(\text{en})_2(\text{bzmH})\text{Cl}]^{2+}$ in a 50% MeOH–water mixture displayed isosbestic points at 505 and 427 nm with $\epsilon = 77.5$ and $27.5 \text{ dm}^3 \text{ mol}^{-1} \text{ cm}^{-1}$, respectively, which compare well both in position and intensity with the aquation reaction of the same carried out in a fully aqueous medium [λ/nm ($\epsilon \text{ dm}^3 \text{ mol}^{-1} \text{ cm}^{-1}$): 500 (79), 429 (28)]. However, at a relatively high percentage of EG and MeOH and at long reaction times the isosbestic points shifted, thereby indicating that both the solvent components ($\text{H}_2\text{O}/\text{EG}$ or MeOH) of the medium compete for the cobalt(III) centre with water predominating during the solvolysis reaction depicted in eqn (1):



where S = solvent. The rate data at various solvent compositions are presented in tables 1–3. The activation parameters, calculated by the least-squares fitting of the rate data¹ to the transition-state equation:

$$\ln k_{\text{obs}}^s = (\ln k/h + \Delta S^\ddagger/R) - (10^{-3} \Delta H^\ddagger/R) \times (10^3/T) \quad (2)$$

are collected in table 4.

Variation of Rate with Solvent Composition

The observed pseudo-first-order rate constant (k_{obs}^s) decreases with increasing amount of organic solvent (see tables 1–3). Also, the plots of $\log k_{\text{obs}}^s$ against the reciprocal of the

Table 1. Rate data for solvolysis of *cis*-[Co(en)₂BCl]²⁺ (B = imH, bzmH) in methanol–water mixtures: [complex]_T = (2–3) × 10⁻³ mol dm⁻³; [HClO₄]_T = 0.01 mol dm⁻³

MeOH (wt %)	<i>X</i> _{MeOH}	<i>k</i> _{obs} ^s /10 ⁻⁵ s ^{-1 a, b}			
		45.0 ± 0.1 °C	50.2 ± 0.1 °C	55.1 ± 0.1 °C	59.8 ± 0.1 °C
0.00	0.00	1.69 ± 0.05	3.20 ± 0.13 (1.26 ± 0.11)	5.53 ± 0.18	8.98 ± 0.28
5.00	0.0287	1.58 ± 0.05	2.95 ± 0.10 (1.25 ± 0.11)	4.87 ± 0.11	7.55 ± 0.24
10.0	0.0588	1.39 ± 0.08	2.60 ± 0.12 (1.02 ± 0.02)	4.32 ± 0.23	6.93 ± 0.22
20.0	0.1233	1.24 ± 0.09	2.24 ± 0.06 (0.83 ± 0.01)	3.54 ± 0.04	5.35 ± 0.20
30.0	0.1942	0.97 ± 0.03	1.80 ± 0.04 (0.63 ± 0.04)	2.63 ± 0.07	3.65 ± 0.10
40.0	0.2727	0.69 ± 0.04	1.15 ± 0.02 (0.50 ± 0.03)	1.72 ± 0.05	2.58 ± 0.09
50.0	0.3600	0.53 ± 0.03	0.87 ± 0.02 (0.34 ± 0.04)	1.24 ± 0.04	1.80 ± 0.05
60.0	0.4576	0.44 ± 0.02	0.72 ± 0.05 (0.30 ± 0.03)	1.01 ± 0.03	1.35 ± 0.04
70.0	0.5675	0.25 ± 0.02	0.42 ± 0.05	0.63 ± 0.04	0.80 ± 0.05
80.0	0.6923	0.16 ± 0.07	0.31 ± 0.05	0.43 ± 0.02	0.54 ± 0.05

^a Values in parentheses at 50.2 °C are for B = imH; all other values are for B = bzmH. ^b Mean value and the error quoted as standard deviation were calculated from 10–15 individual values of *k*_{obs}^s from duplicate or triplicate runs, respectively, at each solvent composition.

Table 2. Rate data for solvolysis of *cis*-[Co(en)₂(imH)Cl]²⁺ in ethyleneglycol–water mixtures: [complex]_T = (2.7–4.0) × 10⁻³ mol dm⁻³; [HClO₄]_T = 0.01 mol dm⁻³

EG (wt %)	<i>X</i> _{EG}	<i>k</i> _{obs} ^s /10 ⁻⁵ s ^{-1 a}			
		50.0 ± 0.1 °C	54.8 ± 0.1 °C	59.7 ± 0.1 °C	64.7 ± 0.1 °C
0.00	0.00	1.21 ± 0.03	2.00 ± 0.05	3.64 ± 0.12	5.51 ± 0.15
5.00	0.015	1.14 ± 0.02	1.86 ± 0.04	3.38 ± 0.09	5.48 ± 0.11
10.0	0.0314	1.07 ± 0.01	1.83 ± 0.06	3.14 ± 0.04	5.17 ± 0.18
20.0	0.0677	0.90 ± 0.02	1.60 ± 0.04	2.74 ± 0.09	4.84 ± 0.16
30.0	0.1106	0.78 ± 0.03	1.38 ± 0.01	2.37 ± 0.06	3.78 ± 0.10
40.0	0.1622	0.62 ± 0.02	1.12 ± 0.04	1.97 ± 0.03	3.28 ± 0.03
50.0	0.2250	0.54 ± 0.02	0.88 ± 0.08	1.72 ± 0.05	2.70 ± 0.13
60.0	0.3034	0.44 ± 0.03	0.83 ± 0.04	1.38 ± 0.03	2.23 ± 0.07
70.0	0.4038	0.36 ± 0.02	0.60 ± 0.04	1.18 ± 0.04	1.65 ± 0.04
80.0	0.5373	0.27 ± 0.01	0.38 ± 0.06	0.88 ± 0.04	1.26 ± 0.03

^a See footnote (b) of table 1.

bulk dielectric constant of the medium⁵ (*D*_s⁻¹) are reasonably good straight lines (correlation coefficient = 0.991–0.996) for the MeOH–water medium; however, such plots for EG–water tend to be curved [fig. 1(a)]. The plots of log *k*_{obs}^s against the revised solvent ionising power of MeOH–H₂O media reported by Bentley and Carter,^{2b} *Y*_{1-AdCl} (1-adamantyl chloride scale), are reasonably linear [fig. 1(b)] at 50 °C (correlation coefficient = 0.997) with slope = 0.23 and 0.25 for imidazole and benzimidazole complexes, respectively, which agree well with the values of the slopes of analogous plots for the aquation of the halogenoamine cobalt(III) complexes in relatively water-rich alcohol–water media.^{1,6} The plots of log *k*_{obs}^s against the mole fraction of MeOH (*X*_{MeOH}) also generate straight lines for the benzimidazole complex (correlation coefficient = 0.997–0.998) with slopes = -1.42 ± 0.04 to -1.78 ± 0.03 at 45 to 59.8 °C. Similar plots for imidazole complex were also linear for the MeOH–water and EG–water media at 50 and 64.8 °C with slopes of -1.46 ± 0.03 and -1.28 ± 0.03, respectively (correlation

Table 3. Rate data for solvolysis of *cis*-[Co(en)₂(bzmH)Cl]²⁺ in ethylene glycol–water mixtures: [complex]_T = 2.0 × 10⁻³ mol dm⁻³; [HClO₄]_T = 0.01 mol dm⁻³

EG (wt %)	<i>X</i> _{EG}	<i>k</i> _{obs} ^s /10 ⁻⁵ s ⁻¹ ^a			
		45.0 ± 0.1 °C	50.0 ± 0.1 °C	54.9 ± 0.1 °C	64.7 ± 0.1 °C
0.00	0.00	1.69 ± 0.02	3.62 ± 0.12	5.57 ± 0.19	15.20 ± 0.5
5.00	0.015	1.64 ± 0.05	2.88 ± 0.05	4.89 ± 0.07	14.00 ± 0.7
10.0	0.0314	1.46 ± 0.09	2.62 ± 0.09	4.53 ± 0.14	13.10 ± 0.3
20.0	0.0677	1.31 ± 0.09	2.38 ± 0.09	3.97 ± 0.23	11.50 ± 0.6
30.0	0.1106	1.20 ± 0.05	2.09 ± 0.11	3.17 ± 0.11	9.18 ± 0.35
40.0	0.1622	1.01 ± 0.09	1.62 ± 0.07	2.70 ± 0.06	8.04 ± 0.47
50.0	0.2250	0.92 ± 0.08	1.45 ± 0.03	1.96 ± 0.10	6.09 ± 0.19
60.0	0.3034	0.84 ± 0.05	1.15 ± 0.07	1.59 ± 0.11	4.61 ± 0.21
70.0	0.4038	0.62 ± 0.06	0.95 ± 0.05	1.32 ± 0.06	3.40 ± 0.10
80.0	0.5373	0.45 ± 0.07	0.72 ± 0.03	0.95 ± 0.05	2.36 ± 0.09
90.0	0.7232	—	—	—	1.55 ± 0.04

^a See footnote (b) of table 1.**Table 4.** Activation enthalpy, entropy and free-energy data for the solvolysis of *cis*-[Co(en)₂BCl]²⁺ (B = imH, bzmH) in various MeOH–water and ethylene glycol–water mixtures

org ^a (wt %)	MeOH ^b			EG ^b		
	ΔH^\ddagger /kJ mol ⁻¹	ΔS^\ddagger /J K ⁻¹ mol ⁻¹	ΔG^\ddagger ^c /kJ mol ⁻¹	ΔH^\ddagger /kJ mol ⁻¹	ΔS^\ddagger /J K ⁻¹ mol ⁻¹	ΔG^\ddagger ^c /kJ mol ⁻¹
0.00	96.6 ± 1.1	-33 ± 3	107.1 ± 0.1 (109.7 ± 0.2)	96.6 ± 1.1 (95.3 ± 4.2)	-33 ± 3 (-45 ± 13)	107.1 ± 0.1 (110.3 ± 0.1)
5.00	90.6 ± 2.9	-52 ± 9	107.5 ± 0.1 (109.7 ± 0.2)	93.4 ± 5.6 (96.7 ± 3.0)	-44 ± 17 (-41 ± 9)	107.5 ± 0.0 (110.0 ± 0.0)
10.0	91.6 ± 1.9	-50 ± 6	107.8 ± 0.1 (110.2 ± 0.0)	97.7 ± 1.1 (97.4 ± 2.3)	-31 ± 3 (-40 ± 7)	107.7 ± 0.1 (110.1 ± 0.0)
20.0	81.5 ± 2.9	-83 ± 9	108.2 ± 0.1 (110.8 ± 0.0)	95.0 ± 1.3 (106.0 ± 2.4)	-40 ± 4 (-14 ± 9)	108.0 ± 0.1 (110.6 ± 0.1)
30.0	73.9 ± 7.3	-108 ± 22	108.8 ± 0.1 (111.6 ± 0.1)	89.2 ± 4.1 (94.8 ± 3.4)	-60 ± 12 (-50 ± 10)	108.3 ± 0.1 (111.0 ± 0.1)
40.0	73.3 ± 2.0	-113 ± 6	110.0 ± 0.1 (112.2 ± 0.2)	93.5 ± 5.0 (100.0 ± 1.7)	-49 ± 15 (-36 ± 5)	109.0 ± 0.1 (111.6 ± 0.1)
50.0	70.7 ± 2.9	-124 ± 9	110.8 ± 0.1 (113.2 ± 0.2)	83.7 ± 6.8 (99.4 ± 4.8)	-80 ± 20 (-39 ± 15)	109.3 ± 0.1 (112.0 ± 0.1)
60.0	63.1 ± 3.9	-149 ± 12	111.3 ± 0.2 (113.5 ± 0.2)	76.9 ± 7.4 (94.0 ± 4.5)	-102 ± 22 (-57 ± 13)	109.9 ± 0.1 (112.5 ± 0.2)
70.0	65.6 ± 6.4	-146 ± 19	112.7 ± 0.3	77.5 ± 4.5 (93.3 ± 9.5)	-102 ± 13 (-61 ± 28)	110.4 ± 0.1 (113.1 ± 0.1)
80.0	52.0 ± 9.9	-190 ± 30	113.5 ± 0.4	78.0 ± 5.7 (92.8 ± 6.7)	-103 ± 17 (-65 ± 20)	111.2 ± 0.1 (113.8 ± 0.1)

^a Organic solvent component. ^b Parenthesized values are for the imidazole complex; all other values are for the benzimidazole complex. ^c At 323.2 K.

coefficient = 0.998). At all other temperatures the log *k*_{obs}^s vs. *X*_{EG} plots for both the complexes are, however, non-linear. Typical plots are presented in fig. 2. Such non-linear plots are indicative of the specific solvation effects of EG–water medium on the solvolysis rates. However, we are led to believe that the substrate, *cis*-[Co(en)₂BCl]²⁺ (where B = imH or bzmH), presumably does not discriminate between the solvent

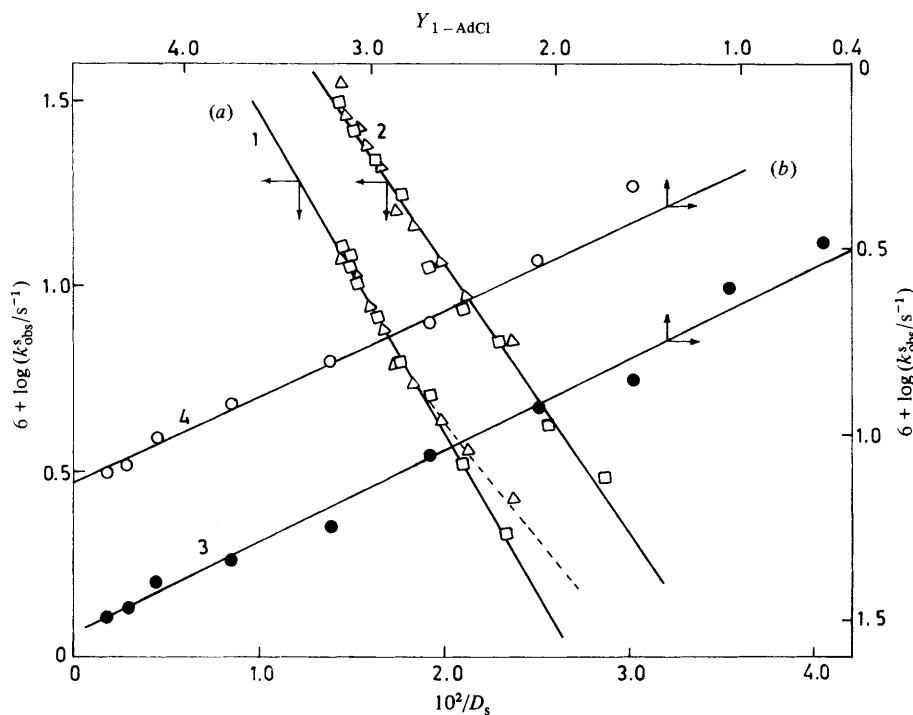


Fig. 1. (a) Plots of $6 + \log(k_{\text{obs}}^s/s^{-1})$ vs. $10^2/D_s$ at 50 °C for (1) the imidazole complex and (2) the benzimidazole complex; \square , MeOH–water; \triangle , EG–water. (b) Plots of $6 + \log(k_{\text{obs}}^s/s^{-1})$ vs. Y_{1-AdCl} (MeOH–water) plots at 50 °C for (3) the imidazole complex and (4) the benzimidazole complex.

components, MeOH or H_2O , in its solvation envelope or skin phase.⁷ Both the initial state and the transition state seem to be solvated by both solvent components without being selective for either MeOH or H_2O . It is most likely that the solvation of the substrates depends upon the dual solvent vectors, *i.e.* the acidity (A_s) and basicity (B_s) parameters⁸ of the solvent mixtures, which for MeOH–water vary linearly with X_{MeOH} over the entire composition range studied [see eqn (4) and (5) of ref. (1)]. The same analysis is also applicable to EG–water medium, for which the assigned values of the acidity and basicity parameters of EG and H_2O ($A_{\text{EG}} = 0.78$, $A_{H_2O} = 1.0$; $B_{\text{EG}} = 0.84$, $B_{H_2O} = 1.0$)⁸ also predict negative slopes of the straight line plot of $\log k_{\text{obs}}^s$ vs. X_{EG} [see eqn (4)–(7) of ref. (1)]. The structural perturbations in this solvent system, however, tend to modulate the solvent cosphere of the substrates, so that the linearity in the $\log k_{\text{obs}}^s$ vs. X_{EG} plot is not maintained over the entire composition range studied. The biphasic nature of the linear plots of $\log k_{\text{obs}}^s$ vs. X_{EG} at higher temperatures for the benzimidazole complex (see fig. 2) is then reconciled with the non-constancy of the parameters l_1 and l_2 of the solvent-effect relationship:

$$\log k_{\text{obs}}^s = l_1 X_{\text{EG}} + l_2 + c$$

[c is a constant; see eqn (7) of ref. (1)] over the entire composition range. Interestingly, l_1 and l_2 are virtually constant for the imidazole complex in the X_{EG} range = 0–0.537 at 64.7 °C, thus reflecting profound thermal effects on the structural perturbations in the EG–water mixtures and the disappearance of the specific effect of solvation on the solvolysis rate at relatively high temperatures.

An excellent linear correlation between $\log k_{\text{obs}}^s(\text{RCl}^{2+})$ and $\log k_{\text{obs}}^s(\text{RBr}^{2+})$ { $\text{R} = [\text{Co}(\text{en})_2(\text{bzmH})]^{3+}$, see ref. (1) for data for the bromo complex} over the whole

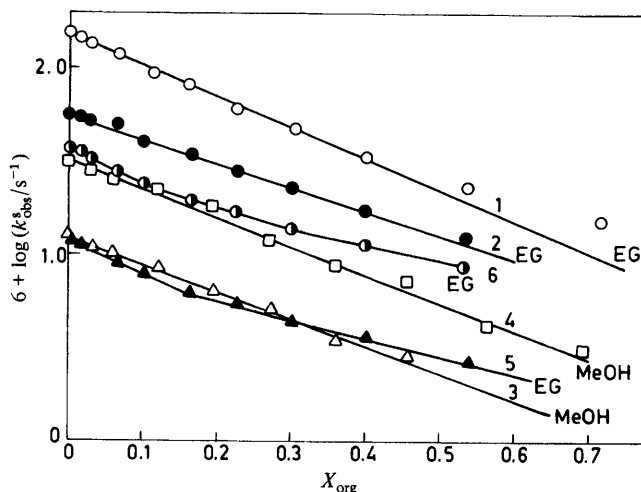
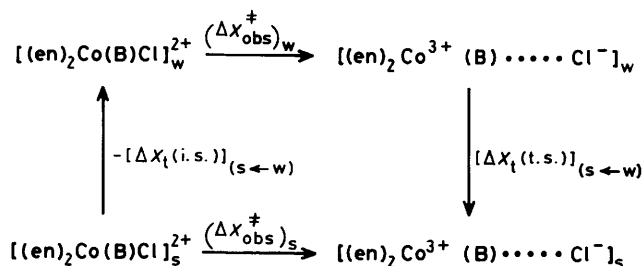


Fig. 2. Plots of $6 + \log(k_{\text{obs}}^s/\text{s}^{-1})$ vs. X_{org} (where X_{org} is the mole fraction of the organic solvent component) for the solvolysis of $\text{cis}[\text{Co}(\text{en})_2(\text{B})\text{Cl}]^{2+}$ [B = benzimidazole for 1 (64.7 °C), 4 and 6 (50 °C); B = imidazole for 2 (64.7 °C), 3 and 5 (50 °C)].



Scheme 1. Dissociative mode of activation; $X = G, H$ or S .

range of solvent compositions, $0 \leq X_{\text{MeOH}} \leq 0.6923$ and at 50 °C with slope = 0.93 ± 0.03 (correlation coefficient = 0.996) can be taken to indicate that there is no change in the mechanism of solvolysis with change in solvent composition. The familiar dissociative interchange mechanism (I_{d}),⁹ in which the Co—Cl bond is stretched to its limit in the transition state may be depicted as in scheme 1. Using the conventional thermodynamic cycle it can be shown that k_{obs}^s and k_{obs}^w (the rate constant in the fully aqueous medium) are related to the free energy of transfer of the transition state, $[\Delta G_{\text{t}}(\text{t.s.})]_{(\text{s} \leftarrow \text{w})}$, and the initial state, $[\Delta G_{\text{t}}(\text{i.s.})]_{(\text{s} \leftarrow \text{w})}$, as given by:

$$\log k_{\text{obs}}^s = \log k_{\text{obs}}^w - (1/2.303RT)[\Delta G_{\text{t}}(\text{t.s.}) - \Delta G_{\text{t}}(\text{i.s.})]_{(\text{s} \leftarrow \text{w})} \quad (3)$$

where transfer of species is assumed to take place from water (w) to the mixed solvent (s). The non-electrostatic component of the relative transfer free-energy term, which is supposed to include all changes in the free energy that result in structural changes in the solvent when the initial state and the transition state of a given complex are transferred from water to the solvent mixtures, do not appear to be sensitive to the solvent composition of the MeOH–water mixture. It is the electrostatic component of the relative transfer free energy which varies linearly (having a negative slope) with the reciprocal of the bulk dielectric constant of the MeOH–water mixture [see fig. 1 (a)]. This is consistent with the fact that the ionization of the Co—Cl bond plays a dominant role

Table 5. Calculated values of the relative transfer thermodynamic functions at 323.2 K

org ^a (wt %)	$[\Delta G_t(\text{t.s.}) - \Delta G_t(\text{i.s.})]_{(\text{s+w})}^b$ /kJ mol ⁻¹		$[\Delta H_t(\text{t.s.}) - \Delta H_t(\text{i.s.})]_{(\text{s+w})}^b$ /kJ mol ⁻¹		$[\Delta S_t(\text{t.s.}) - \Delta S_t(\text{i.s.})]_{(\text{s+w})}^b$ /J K ⁻¹ mol ⁻¹	
	MeOH	EG	MeOH	EG	MeOH	EG
5.00	0.2±0.1 (0.0±0.3)	0.6±0.1 (0.2±0.1)	-6±3	-3±6 (+1±5)	-19±9	-11±17 (+4±13)
10.0	0.5±0.1 (0.6±0.2)	0.9±0.1 (0.3±0.1)	-5±2	+1±1 (+2±4)	-17±7	+2±4 (+5±13)
20.0	0.9±0.1 (1.1±0.2)	1.1±0.1 (0.8±0.1)	-15±3	-2±1 (+11±5)	-50±9	-7±5 (+31±15)
30.0	1.5±0.1 (1.9±0.2)	1.5±0.1 (1.2±0.1)	-23±2	-7±4 (-0.5±5)	-75±22	-27±12 (-5±13)
40.0	2.7±0.1 (2.5±0.2)	2.2±0.1 (1.8±0.1)	-23±3	-3±5 (+5±4)	-80±7	-16±15 (+9±13)
50.0	3.5±0.1 (3.5±0.2)	2.5±0.1 (2.2±0.1)	-26±3	-13±7 (+4±6)	-91±9	-47±20 (+6±16)
60.0	4.0±0.2 (3.9±0.2)	3.1±0.1 (2.7±0.1)	-33±4	-20±7 (-1±5)	-116±12	-69±22 (-12±18)
70.0	5.4±0.3	3.6±0.1 (3.2±0.1)	-31±7	-19±5 (-2±10)	-113±19	-69±13 (-16±28)
80.0	6.3±0.4	4.3±0.1 (4.0±0.1)	-45±10	-19±6 (-2±8)	-157±30	-70±17 (-20±23)

^a Organic solvent component. ^b Parenthesized values are for the imidazole complex; all other values are for the benzimidazole complex.

in the activation process. The observed non-linearity in the plot of $\log k_{\text{obs}}^s$ vs. D_s^{-1} for EG–water mixtures, in contrast to eqn (3), may be attributed to (i) failure of both the point-charge model of the complex ions and the dielectric-continuum model of the reaction media and (ii) a presumably non-linear variation of the non-electrostatic component of the relative transfer free-energy term, $[\Delta G_t(\text{t.s.}) - \Delta G_t(\text{i.s.})]_{(\text{s+w})}$ with the solvent composition.

The values of the relative transfer free-energy term at 50 °C [calculated using eqn (3)] are presented in table 5. For both complexes it is positive, with a steadily increasing magnitude as X_{org} increases. These data are consistent with the fact that the stabilizing effect of the medium on the initial state is much greater than that on the transition state, the free energy of transfer for both the transition state and the initial state being assumed to be either negative or positive. The free energy of transfer of several cations from water to MeOH–water mixtures are reported to be positive or negative, depending on the nature of the cation (with respect to the charge and ligand environment) and the different approximations used.^{10–12} The transfer free-energy data for the crystal violet cation [$\Delta G_t(\text{CV}^+)$ at 25 °C] reported by Kundu *et al.*¹³ for EG–water and MeOH–water mixtures also reflect that this bulky cation with hydrophobic groups $\{\text{CV}^+ = [(\text{CH}_3)_2\text{NC}_6\text{H}_4]_3\text{C}^+\}$ is relatively less stabilized in the former solvent. The values of the relative transfer free energy are more positive for the benzimidazole complex than for the imidazole complex at any solvent composition for the EG–water system. This leads us to believe that the solvation changes associated with both the initial state and the transition state are sensitive to the nature of the non-labile ligands imH and bzmH; the relatively bulkier and more hydrophobic benzimidazole probably destabilizes the I_a transition state in EG–water mixtures to a greater extent than imidazole (*i.e.* $[\Delta G_t(\text{t.s.})]_{(\text{s+w})}(\text{bzmH}) > [\Delta G_t(\text{t.s.})]_{(\text{s+w})}(\text{imH})$). Wells¹⁴ assumes a fully

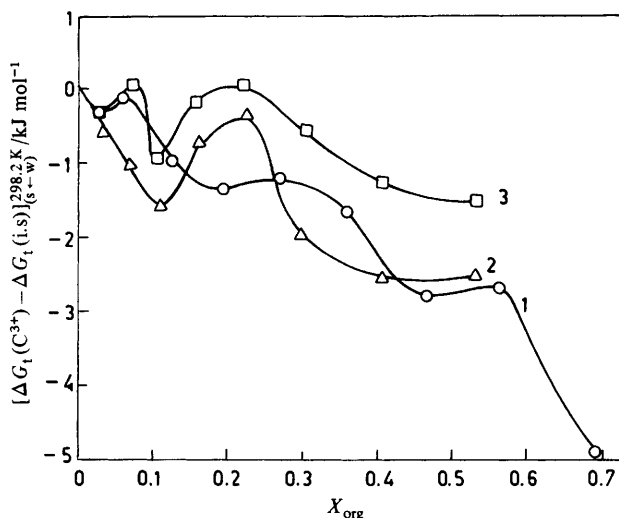


Fig. 3. Dependence of the free energy of transfer $[\Delta G_t(C^{3+})]_{(s\leftarrow w)}$ of $cis\text{-}[\text{Co}(\text{en})_2\text{B}]^{3+}$ * relative to that of $cis\text{-}[\text{Co}(\text{en})_2\text{BCl}]^{2+}$ at 25 °C as a function of X_{org} : (1) bzmH (MeOH–water), (2) bzmH (EG–water), (3) imH (EG–water).

dissociative transition state (D mechanism)⁹ in order to analyse the solvent effects on the solvolytic aquation of several chloroamine cobalt(III) complexes. The additivity principle may then be assumed to be valid for the transfer free energy of the transition state to yield

$$[\Delta G_t(\text{t.s.})]_{(s\leftarrow w)} = [\Delta G_t(C^{3+})]_{(s\leftarrow w)} + [\Delta G_t(\text{Cl}^-)]_{(s\leftarrow w)} \quad (4)$$

where $[\Delta G_t(C^{3+})]_{(s\leftarrow w)}$ denotes the transfer free energy of the dissociative transition state, $C^{3+} = \{cis[\text{Co}(\text{en})_2(\text{bzmH})]\}^*$. The values of the relative transfer free-energy term $[\Delta G_t(C^{3+}) - \Delta G_t(\text{i.s.})]_{(s\leftarrow w)}$ at 25 °C were calculated from eqn (5), obtained by combining eqn (3) and (4), using the extrapolated values of the rate constants and the values of $[\Delta G_t(\text{Cl}^-)]_{(s\leftarrow w)}$ reported by Abraham *et al.*¹⁰ (for MeOH–water, after conversion to the mole fraction scale¹²) and Kundu *et al.*¹³ [for EG water; values of $[\Delta G_t(\text{Cl}^-)]_{(s\leftarrow w)}$ on the mole fraction scale were obtained by interpolation of the data available wherever necessary]. The values of $[\Delta G_t(C^{3+}) - \Delta G_t(\text{i.s.})]_{(s\leftarrow w)}$ were found to be negative for MeOH water at all compositions; for the EG–water system the values of this term were also negative and decreased non-linearly (see fig. 3) at a higher percentage of EG. This indicates a relatively strong propensity of the tripositive cobalt(III) species (C^{3+}) to solvation, as do solvent structural changes associated with the transfer of the ionic species from the aqueous medium to the mixed solvent:

$$[\Delta G_t(C^{3+}) - \Delta G_t(\text{i.s.})]_{(s\leftarrow w)} = 2.303RT \log(k_{\text{obs}}^w/k_{\text{obs}}^s) - [\Delta G_t(\text{Cl}^-)]_{(s\leftarrow w)}. \quad (5)$$

The transfer free-energy calculations also show that the tripositive cobalt(III) species (C^{3+}) is more solvated in the alcohol-rich region of the mixed solvent than in water. However, this does not lead to rate enhancement, since the positive values of $[\Delta G_t(\text{Cl}^-)]_{(s\leftarrow w)}$ tip the balance in favour of rate retardation with increasing X_{org} .

Variation of Activation Enthalpy and Entropy with Solvent Composition

Fig. 4 and 5 and data in table 4 depict the variation of the activation enthalpies and entropies (ΔH^\ddagger and ΔS^\ddagger) with X_{org} . The maxima and minima in the plots of ΔX^\ddagger vs. X_{org} ($X = H, S$) at $X_{\text{org}} < 0.15$ and the non-linear decreasing trend in these parameters

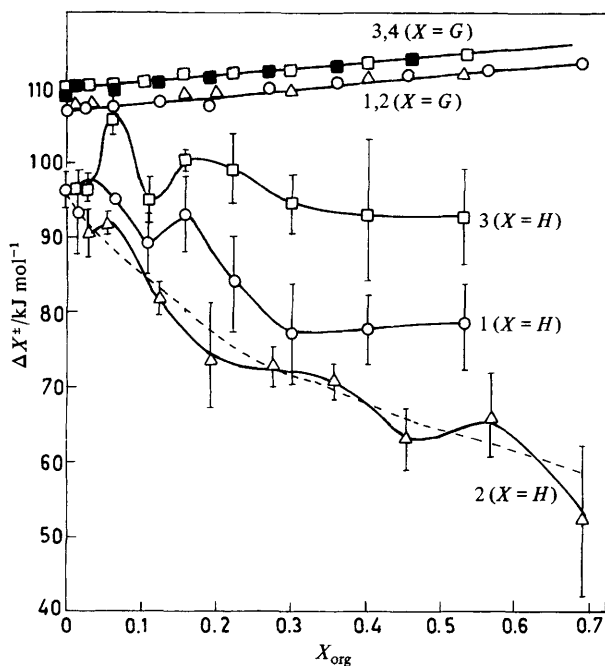


Fig. 4. Dependence of the activation free energy (ΔG^\ddagger) and activation enthalpy (ΔH^\ddagger) of solvolysis of *cis*-[Co(en)₂BCl]²⁺ (B = bzmH, imH) on the mole fraction of EG and MeOH; ΔG^\ddagger is at 323.2 K. (1) bzmH (EG–water), (2) bzmH (MeOH–water), (3) imH (EG–water) and (4) imH (MeOH–water).

beyond this mole fraction of EG and MeOH show that the solvent structural perturbations significantly modulate the values of these parameters. The values of the relative transfer thermodynamic functions $[\Delta X_i(t.s.) - \Delta X_i(i.s.)]_{(s-w)}$ ($X = H, S$) (see table 5) are also related to solvent structure. The relative transfer entropy and enthalpy at any value of X_{EG} are sensitive to the nature of the non-labile ligand, imH and bzmH; the values of these parameters for the imidazole complex are distinctly more positive than the corresponding values for the benzimidazole complex. However, ΔG^\ddagger (323.2 K) increases linearly with X_{org} over the entire composition range; the data points for a given complex and for both solvent systems fit the same straight line reasonably well. Evidently the rate-enhancing effect due to the decreasing value of ΔH^\ddagger is offset by the large negative value of ΔS^\ddagger . To a large extent, the effects of ΔH^\ddagger and ΔS^\ddagger on the rate are mutually compensatory (see fig. 6). The large negative values of ΔS^\ddagger being consistent with stereoretentive solvolysis¹⁵ corroborates the fact that the transition state is much more solvated than the initial state. The substrates under investigation possess a potentially acidic NH group ($pK_{NH} = 8.6$ and *ca.* 10 for the coordinated benzimidazole and imidazole, respectively^{3,16}) adjacent to the reaction site (*i.e.* the Co–Cl dipole), and since the methyl group and the bulky benzimidazole species can take part in hydrophobic association¹⁷ we believe that solvation in the initial and transition states will involve cooperative hydrogen bonding in which the solvent molecules, Co–Cl and N–H dipoles of the imidazole or benzimidazole ligands take part as depicted in fig. 7. [Note that the model of front-side solvation was postulated by Adamson and Basolo¹⁸ in the context of the aquation of $(NH_3)_5CoCl^{2+}$.] This effect is likely to be strengthened at the NH site in the transition state, since development of positive charge at the cobalt(III) centre will accentuate the dipole–dipole interaction. A similar situation involving EG

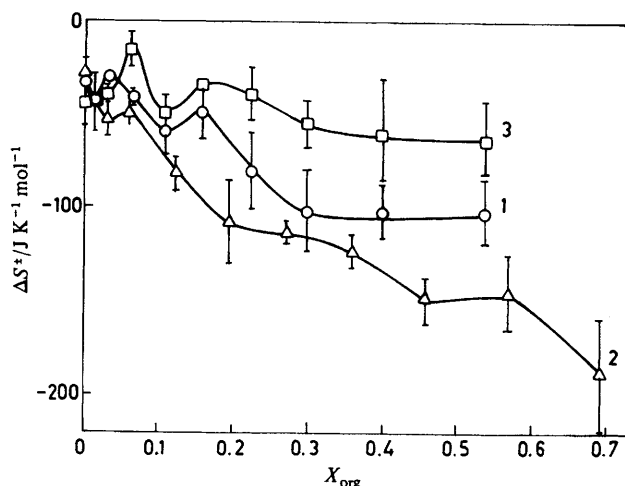


Fig. 5. Dependence of the activation entropy of the solvolysis of $\text{cis-}[\text{Co}(\text{en})_2\text{BCl}]^{2+}$ (B = bzmH, imH) on the mole fraction of EG and MeOH. (1) bzmH (EG-water), (2) bzmH (MeOH-water) and (3) imH (EG-water).

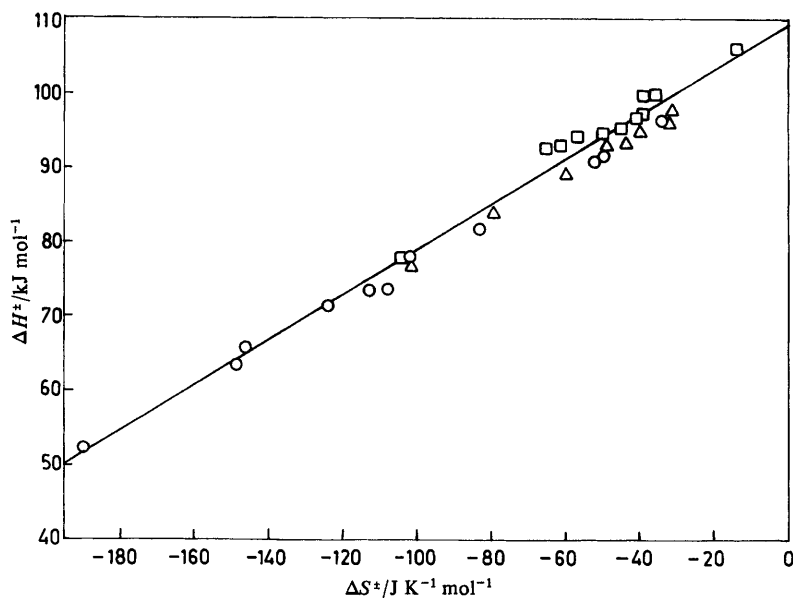


Fig. 6. Plot of ΔH^\ddagger kJ mol^{-1} against ΔS^\ddagger $\text{J K}^{-1} \text{mol}^{-1}$: ○, bzmH (MeOH-water); △, bzmH (EG-water); □, imH (EG-water).

molecules probably prevails in EG-water mixtures, and presumably the initial and transition states are preferentially solvated by EG, since it can effectively participate in hydrogen bonding with the NH and Co-Cl dipoles by utilizing both of its OH groups. In this context one should note the relatively more positive values of ΔS^\ddagger ($\Delta S^\ddagger_{\text{EG-water}} > \Delta S^\ddagger_{\text{MeOH-water}}$, see table 4) at all compositions of EG-water for the benzimidazole complex.

Furthermore, the large decrease of ΔH^\ddagger with increasing X_{MeOH} for $\text{cis-}[\text{Co}(\text{en})_2\text{-}(\text{bzmH})\text{Cl}]^{2+}$ (see fig. 4 and table 4) reflects the energetic role of the solvent cosphere of

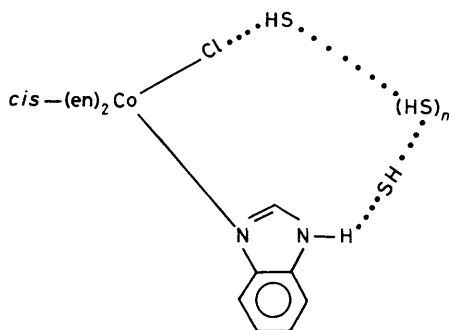


Fig. 7. Front-side initial state solvation in which SH is MeOH, H₂O or EG.

this complex in indirectly influencing the development of the highly polar transition state. The overall values of ΔH^\ddagger and ΔS^\ddagger may be taken to be composites of the reaction component and the solvational component¹⁹ ($\Delta X_{\text{overall}}^\ddagger = \Delta X_{\text{R}}^\ddagger + \Delta X_{\text{S}}^\ddagger$). The validity of the compensation law (see fig. 6) is therefore in keeping with the fact that perturbations of the reaction zone and the solvent network remain proportional to each other with increasing X_{org} , so that the isodelphic and the lyodelphic components of ΔH^\ddagger and ΔS^\ddagger correlate well with each other over the entire composition range of both the solvent systems used.²⁰

This work was supported by a grant from CSIR to A. C. D. N. D. thanks the CSIR for a Junior Fellowship.

References

- 1 Part 1: A. C. Dash and N. Dash, *J. Chem. Soc., Faraday Trans. 1*, 1987, **83**, 2505.
- 2 (a) E. Grunwald and S. Winstein, *J. Am. Chem. Soc.*, 1948, **70**, 846; (b) T. W. Bentley and G. E. Carter, *J. Am. Chem. Soc.*, 1982, **104**, 5741.
- 3 A. C. Dash and S. K. Mohapatra, *J. Chem. Soc., Dalton Trans.*, 1977, 1207.
- 4 I. J. Kindred and D. A. House, *Inorg. Chim. Acta*, 1975, **14**, 185.
- 5 G. Akerlof, *J. Am. Chem. Soc.*, 1932, **54**, 4125.
- 6 J. Burgess and M. G. Price, *J. Chem. Soc. A*, 1971, 3108 and references therein; G. Thomas and L. A. P. Kane-Magurie, *J. Chem. Soc., Dalton Trans.*, 1974, 1688.
- 7 B. G. Cox, G. R. Hedwig, A. J. Parker and D. W. Watts, *Austr. J. Chem.*, 1974, **27**, 477; A. J. Parker, *Electrochim. Acta*, 1976, **21**, 671.
- 8 C. G. Swain, M. S. Swain, A. L. Powell and S. Alunni, *J. Am. Chem. Soc.*, 1983, **105**, 502.
- 9 C. H. Langford and H. B. Gray, *Ligand Substitution Processes* (W. A. Benjamin, New York, 1965).
- 10 M. H. Abraham, T. Hill, H. C. Ling, R. A. Schulz and R. A. Watt, *J. Chem. Soc., Faraday Trans. 1*, 1984, **80**, 489.
- 11 C. F. Wells, *J. Chem. Soc., Faraday Trans. 1*, 1973, **69**, 984.
- 12 M. J. Blandamer, J. Burgess, B. Clark, P. P. Duce, A. W. Hakin, N. Gosal, S. Radulovic, P. Guardado, F. Sanchez, C. C. Hubbard, Ezz-E. A. Abu-Gharib, *J. Chem. Soc., Faraday Trans. 1*, 1986, **82**, 1471.
- 13 U. Mendal, S. Sen, K. Das and K. K. Kundu, *Can. J. Chem.*, 1986, **64**, 300; A. K. Das and K. K. Kundu, *Ind. J. Chem., Sect. A*, 1978, **16**, 467.
- 14 A. E. Eid and C. F. Wells, *J. Chem. Soc., Faraday Trans. 1*, 1985, **81**, 1401.
- 15 M. L. Tobe, *Inorg. Chem.*, 1968, **7**, 1260.
- 16 A. C. Dash, M. S. Dash and S. K. Mohapatra, *J. Chem. Res.*, 1979, (S) 354; (M) 4531.
- 17 F. Franks, *Water—A Comprehensive Treatise*, ed. F. Franks (Plenum Press, New York, 1973), vol. 4, p. 1.
- 18 A. W. Adamson and F. Basolo, *Acta Chem. Scand.*, 1955, **9**, 1261.
- 19 M. J. Blandamer, *Adv. Phys. Org. Chem.*, 1977, **14**, 247.
- 20 E. Grunwald, *J. Am. Chem. Soc.*, 1984, **106**, 5414.